Hindawi
International Journal of Antennas and Propagation
Volume 2023, Article ID 8477138, 12 pages
https://doi.org/10.1155/2023/8477138

Research Article

Fabrication of a Flexible RFID Antenna by Using the Novel Environmentally Friendly Additive Process

Pandi Divya and Wen-Hsi Lee

Department of Electrical Engineering, National Cheng Kung University, Tainan, Taiwan

Correspondence should be addressed to Wen-Hsi Lee; leewen@mail.ncku.edu.tw

Received 6 April 2023; Revised 13 August 2023; Accepted 28 August 2023; Published 27 September 2023

Academic Editor: Rakesh Chowdhury

Copyright © 2023 Pandi Divya and Wen-Hsi Lee. This is an open access article distributed under the Creative Commons Attribution License, which permits unrestricted use, distribution, and reproduction in any medium, provided the original work is properly cited.

The fabrication of flexible antennas for RFID applications can be divided into subtractive and additive methods. In this study, a low-cost additive method is proposed, which involves printing aluminum paste and utilizing a galvanic replacement reaction. Through a galvanic replacement process, copper sulfate waste effluent was employed to convert the aluminum electrode into a highly conductive copper electrode. The physical characteristics of the Cu electrode, such as surface flatness, thickness, and Al-Cu conversion ratio, were studied. The Cu electrode, produced using an innovative additive technique at a temperature of 75°C for 15 minutes, exhibits the lowest resistivity of 5.89×10^{-8} Ωm. This resistivity is comparable to that of a commercial silver thick film electrode, making it suitable for use in manufacturing RFID antennas for RFID module applications. With an S_{11} of −40 dB at 1.26 GHz, a maximum gain of 2.87 dBi, a maximum efficiency of 53.63%, and a reading distance of 9 meters, the RFID module demonstrates impressive performance. The reading distance of an RFID module with a copper foil antenna is longer (8.5 meters).

1. Introduction

An RFID system comprises three components: an antenna, a transceiver (often combined into one reader), and a transponder (the tag) [1, 2]. The conventional RFID antenna process uses copper clad laminate (CCL) or flexible copper clad laminate (FCCL) with exposure and etching processes, which not only causes a large amount of copper waste and copper scrap but also generates agent and developer waste during the process to be harmful to the environment. The main motive of this work to alter FPCB (fabricated printed circuit board) for RFID antennas now uses the additive process rather than the conventional subtractive method, which significantly decreases the trash and sewage produced by the subtraction process [3, 4].

When utilized as substrates for fabricating flexible antennas, flexible PET (polyethylene terephthalate) sheets encounter two significant challenges in additive manufacturing: low-temperature heat treatment and high conductivity of the conductive paste [5]. The primary additive method currently in use involves screen printing thick layers of silver (Ag) or copper (Cu) pastes, followed by thermal treatment of those pastes in either an air or nitrogen atmosphere. However, the cost of producing thick film silver paste or copper paste is high. In this work, a cost-effective aluminum paste is used in place of the prohibitively expensive nanosilver paste and other copper paste substitutes that are typically used in classic thick film processes [6, 7]. The most abundant metal on Earth (after silicon and oxygen) is aluminum, which is printed onto a flexible PET substrate sheet using an epoxy resin paste [8, 9]. However, since the Al paste with epoxy resin is nonconductive, the thick film aluminum electrode, which was screen printed and had a higher oxidation potential, was immersed in an aqueous solution of $CuSO_4$ for a certain duration. Then, through a process known as galvanic displacement oxidation-reduction, the metal aluminum was replaced by the metal copper, which has a higher reduction potential [10]. Our work differs significantly from previous research in which not only has Al replaced with Cu on the surface but also aim to replace Al with Cu internally to the greatest extent feasible, replaced with Cu internally. This is due to the porous structure of the dried aluminum paste with epoxy. The formation of a highly conductive Cu layer without electroplating is then achieved by performing a galvanic displacement reaction between Al paste and $CuSO_4$ solution with various additions. Following a galvanic displacement reaction, the performance of the Cu conductor, including roughness, conductivity, and the conversion ratio of Cu/Al, is significantly influenced by the additions in the $CuSO_4$ solution. By the way, cutting-edge circular economy technology is proposed to create flexible substrates for antennas by using the copper sulfate waste produced by the semiconductor industry upstream to perform a galvanic displacement reaction [11]. To achieve high performance of RFID tag antenna on flexible PET substrate, the Al electrode will be completely transformed into a Cu electrode via the galvanic displacement reduction-oxidation reaction. Therefore, in this study, a low-cost and environmentally friendly method was used to fabricate and verify the RFID tag antenna performance [12].

2. Experimental Procedure

Figure 1 shows the experimental flows for this study.

In this study, the PET substrate utilized was sourced from Kolon Industries Inc. The conductive aluminum paste employed was obtained from Li-Cheng Inc. Initially, the PET substrate samples underwent a screen printing process using a thick film aluminum paste. Screen printing, which involves the application of paste through a mesh onto a surface, was employed in this procedure. The printed samples were subsequently subjected to a drying period of approximately 30 minutes at a temperature of 200°C. Following that, an aqueous solution of $CuSO_4$. $5H_2O$(s) (100 g/l) and 98% H_2SO_4 (aq) (50–60 g/l) was prepared for the subsequent displacement reaction. The pH of the $CuSO_4$ (aq) solution was maintained at 0.07. Subsequently, the samples were immersed in a $CuSO_4$ solution and placed on a hot plate. The temperature of the solution was carefully controlled within a range of 45°C–75°C, and the samples were subjected to varying time intervals between 5 minutes and 50 minutes to carry out the galvanic chemical displacement reaction. In order to improve the copper deposition during the displacement reaction, organic additives were also used. Suppressor-type additives were introduced to the $CuSO_4$ solution to study their impact on the kinetics of Cu reduction, whereas accelerators were seen to accelerate the deposition rate. In a future publication, a thorough analysis of the effects of various additives will be presented. Overall, as depicted in Figure 1, this experimental approach was demonstrated, and various phases were stated. The physical properties of Cu electrode on PET film after galvanic displacement reaction including thickness and roughness are examined by using an optical microscope and scanning electron microscope. SJ-210 Mitutoyo uniformity analyzer was used to measure the surface flatness (Ra) of the surface of Cu electrode after galvanic displacement reaction. Multiple spots were used to measure and calculate the sample copper surface's average flatness (Ra) value.

The electrochemical dc polarization measurements were conducted using a potentiostat/galvanostat (Princeton Applied Research PARSTAT model 2273). Resistance of Cu electrode after displacement reaction was measured using a two-probe LCR meter. The resistivity of Cu electrode is calculated based on the formula given as follows, where ρ represents the resistivity, L represents the length, and A represents the area.

$$R = \rho \frac{L}{A}. \tag{1}$$

While tag antenna return loss is measured by vector network analyzers, the reading distance of the tag antenna by RFID readers and the antenna radiation pattern and efficiency are measured by the anechoic chamber's far-field measurement.

3. Results and Discussion

In this section, the influence of solutions temperature and immersed time on the microstructure and electrical properties of the electrodes after replacing aluminum with copper sulfate are discussed.

3.1. Electrochemical Analysis. In this study, the reduction-oxidation substitution reaction of aqueous Cu^{2+} reacts with the aluminum metal to yield Al^{3+} and copper metal, as illustrated in Figure 2(a). The basis for this approach is the effect of organic additives on the kinetics of Cu reduction; accelerator-type additions accelerate deposition while suppressor-type additives slow it down [13].

The potentiodynamic (PD) polarization scans were carried out in electrochemical impedance spectroscopy (EIS) to characterize the properties of the copper sulfate solution with and without additives for the redox reaction as shown in the following equation:

$$2Al + 3Cu^{2+} \longrightarrow 3Cu + 2Al^{3}. \tag{2}$$

3.1.1. Polarization Curve. Using electrochemical analysis to examine the solution, a polarization curve is depicted in Figure 2(b), illustrating that the corrosion current of the electrode escalates with increasing temperature. During Cu electroplating, the Cu ions oxidize from the Cu anode and reduce to deposit on the Cu Cathode. With increasing temperature, a decrease in both cathodic and anodic currents is observed. When the temperature rises, the rate of corrosion and inhibition efficiency (IE) rises. Compared to Ag/AgCl, oxidation significantly improved the efficiency of copper deposition at various temperatures in terms of inhibitory effect. Temperature significantly influences the replacement rate because the amount of corrosion current is directly proportional to the rate of reaction. The temperature of 75°C has the highest inhibition efficiency, and the preferred current density for generating a copper deposition with substantial current efficiency was 0.25–1.5 A/dm^2. As a result, this demonstrates that copper can be effectively

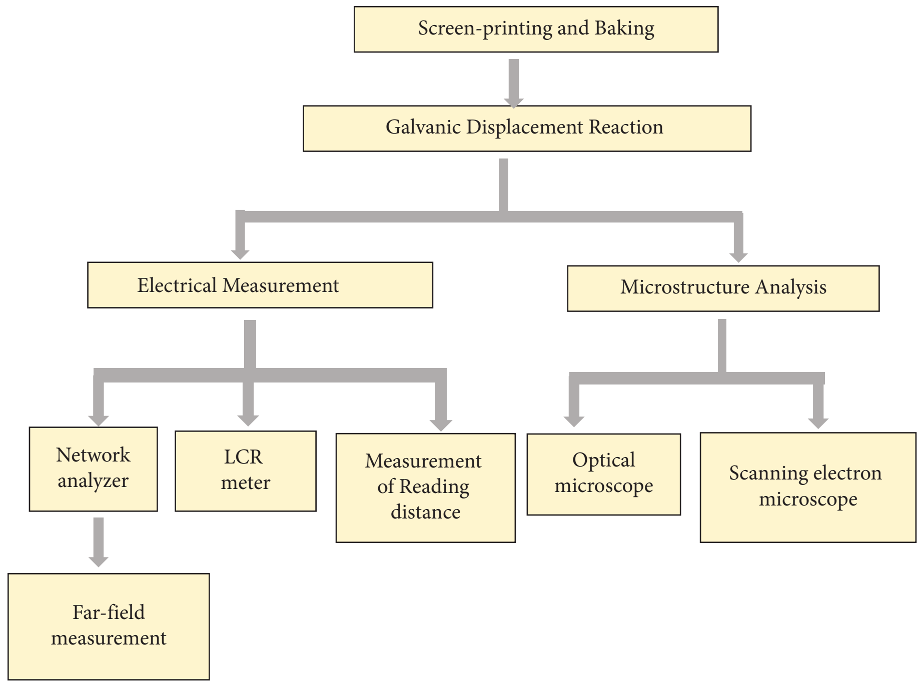

FIGURE 1: Design flowchart for this experiment.

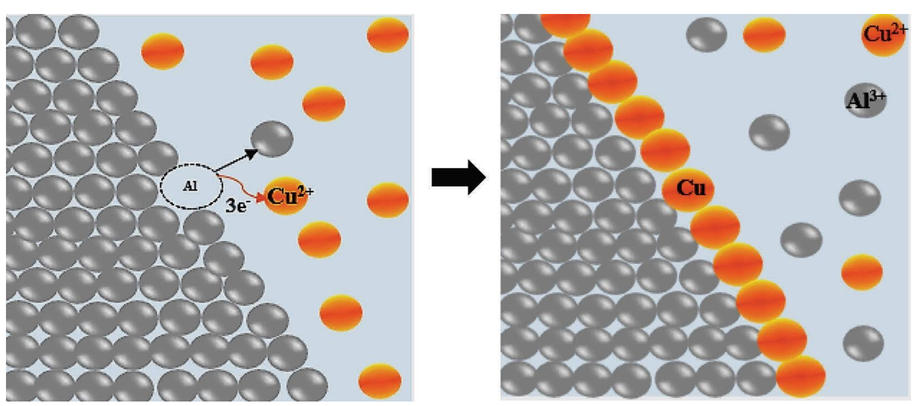

(a)

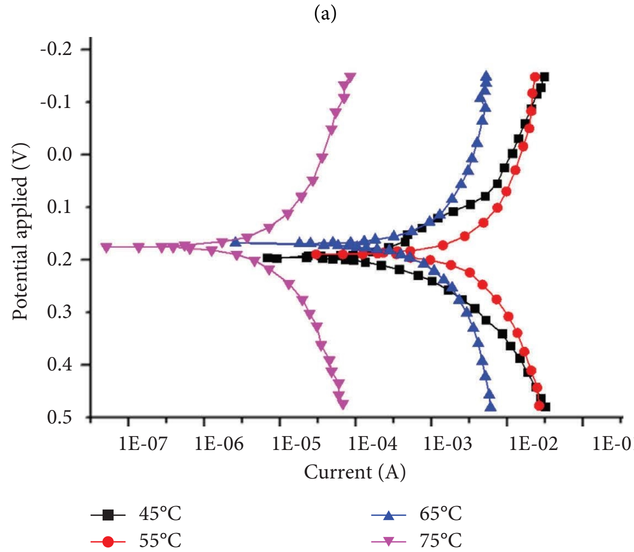

(b)

FIGURE 2: (a) Redox reaction of the Al metal with aqueous Cu^{2+} ions and (b) linear polarization at different temperatures.

deposited on the surface of the aluminum electrode, preventing corrosion of the aluminum.

Figure 3 shows the thickness of copper electrode after galvanic displacement reaction at different solution temperatures with different immersed times. At a lower solution temperature of 45°C, the thickness of Cu electrode gradually increases with increasing immersed time.

On the contrary, at a higher solution temperature of 75°C, the thickness of the Cu electrode increases dramatically within 5 minutes of immersion. However, the thickness of the Cu electrode does not show significant changes when the immersion time is increased beyond that. The minimum thickness of the copper electrode is 22.2 μm after a galvanic displacement reaction at 45°C for 5 minutes. When the solution temperature is increased to 75°C, the maximum thickness of the copper electrode is approximately 27.4 μm, and the flatness is approximately 3 μm after a galvanic displacement reaction for 15 minutes.

Figure 4 shows that the proportion of the Al electrode replaced by Cu electrode increases as the temperature gradually rises. When the solution temperature exceeds 55°C, the replacement ratio of Cu/Al gradually increases as the temperature rises. However, the proportion of replacement significantly decreases with increasing temperature when the replacement time exceeds 30 minutes. Figure 5 shows the scanning electron microscope (SEM), optical microscopy, and cross-section of the sample and cross-section of the sample surface at different temperatures of solution for 15 min. In comparison with the traditional method of using copper foil for antennas, the sample surface exhibited erratic and abnormal growth at a lower temperature. At a higher solution temperature, a smooth surface of the desired thickness of Cu was observed. Figure 5 illustrates that at a high temperature of 75°C, the SEM analysis revealed a dense and smooth surface of copper, resulting in a bright surface appearance.

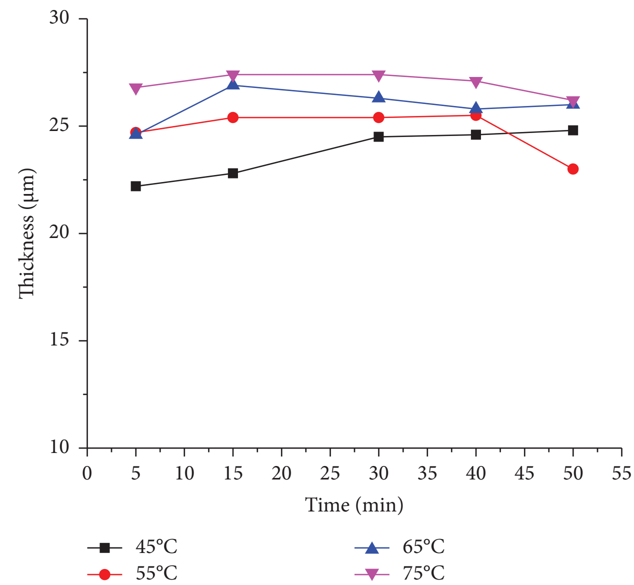

Figure 3: Copper deposition depth at different replacement conditions.

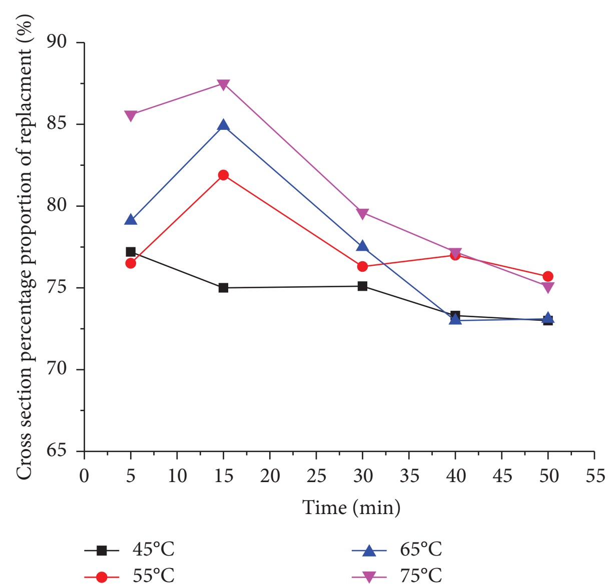

Figure 4: Cross section percentage proportion of replacement at different conditions.

3.2. Measurement of Electrical Property

3.2.1. Resistivity of Cu Electrode. Since aluminum paste contains aluminum powder, resin, and glass powder, it is not possible to replace the entire aluminum electrode with a pure copper electrode by a galvanic displacement reaction. Therefore, this section discusses the difference between the resistivity of the copper electrodes replaced by the replacement method and the resistivity of thick film copper sintered in an N_2 atmosphere [14], as shown in Figure 6.

Table 1 shows the resistance and resistivity of the Cu electrodes after the replacement reaction at various solution temperatures and immersion durations. Figure 6 shows that the resistance decreases with an increase in solution temperature, and the resistance decreases significantly after 15 minutes of immersion time. From Table 1, the resistivity decreases as the solution temperature increases from 45°C to 75°C for the same immersion time of 15 minutes. The lowest resistivity is 5.89×10^{-8} Ωm at 75°C for 15 minutes, which is achieved by the thick film of Cu electrode sintered in a nitrogen atmosphere. The smooth surface and dense microstructure of the copper used to replace aluminum in the copper sulfate solution at 75°C for 15 minutes are favorable factors contributing to the resistivity.

3.2.2. RFID Tag Antenna Characteristics. In this study, the RFID antenna is typically a printed dipole antenna (half-wavelength) with a meander line for UHF RFID (300 MHz–3 GHz) applications [15]. The design was altered to have a maximum 91.75 × 6 millimeter footprint area and was adapted from a previous article [16], as illustrated in Figure 7(a). In comparison to HF tags, the UHF RFID band offers a reading distance with a 1.25 mm spacing and a reading range of up to 12 meters. For applications requiring 980 MHz, it is appropriate. The dipole antenna is the

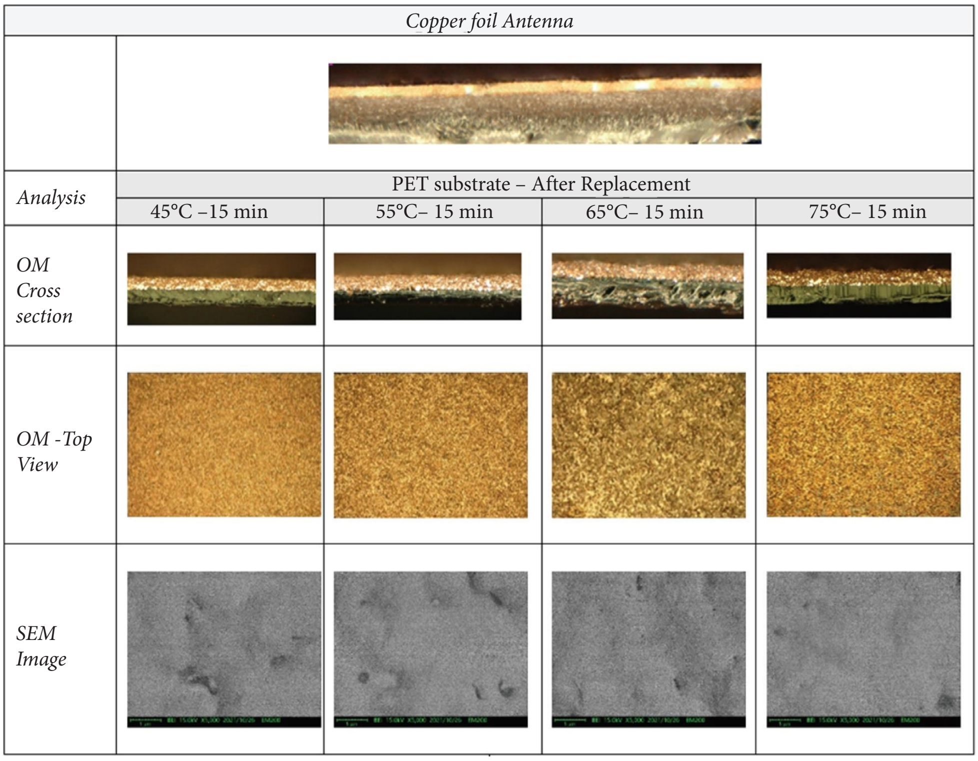

Figure 5: Additive method PET antenna of the replacement condition in comparison with copper foil antenna.

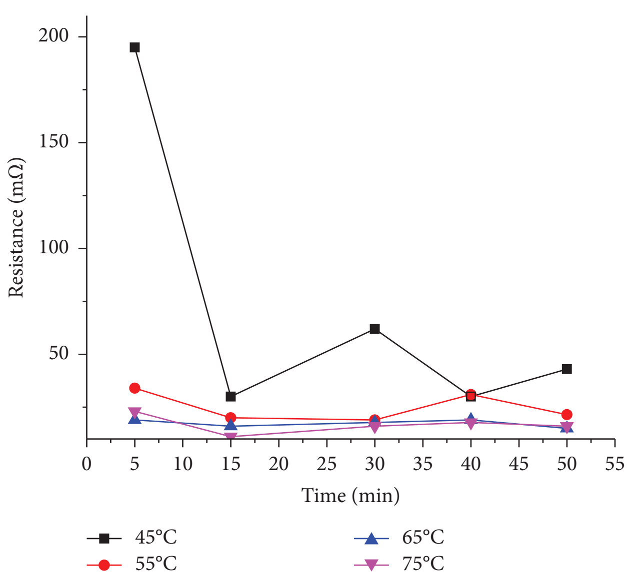

Figure 6: Resistance value of the PET antenna sample after replacement.

Table 1: Resistivity after displacement reaction at different temperature and time.

Temperature Time (min)	Resistivity (Ωm) 45°C	55°C	65°C	75°C
5	7.8×10^{-7}	1.46×10^{-7}	7.7×10^{-8}	8.3×10^{-8}
15	9.9×10^{-8}	8.39×10^{-8}	6.88×10^{-8}	$\mathbf{5.89 \times 10^{-8}}$
30	2.02×10^{-7}	8.36×10^{-8}	7.87×10^{-8}	6.84×10^{-8}
40	1.35×10^{-7}	1.3×10^{-7}	7.23×10^{-8}	7.3×10^{-8}
50	1.89×10^{-7}	9.9×10^{-8}	7.04×10^{-8}	7.7×10^{-8}

The bold value indicates the lowest resistivity in these studies.

earliest and most basic structural form of antenna used in radio communications. It is composed of two symmetrical conductors that are connected to a feeder wire at each end. The simulation results of the return loss (S11) and 3D radiation pattern for the half-wavelength dipole antenna with a meander line are shown in Figures 7(b) and 7(c), respectively. An axially symmetric radiation field is produced by the antenna [17].

The techniques used to fabricate RFID antennas for UHF band applications are contrasted in Figure 8 and Table 2. We compare a novel additive procedure that utilizes the galvanic displacement reaction of PET film to the conventional subtractive method, which involves etching copper foil. Comparative images of RFID dipole antennas created using various techniques are shown in Figures 9(a) and 9(b). The subtractive method, using the etching process, was employed to create Figure 9(a), while the additive method, involving printing and galvanic displacement reaction, was utilized to fabricate Figure 9(b). The fabrication procedures were carried out at different temperatures and for varying durations. The novel additive method is undoubtedly preferable to the subtractive method in terms of reducing the usage of Cu material. The performances of RFID tag antennas created via the subtractive approach with an etching process and the additive method with printing and a galvanic displacement reaction at 75°C for 5–15 minutes are shown in Figures 10(a)–10(d). In the far-field measurement

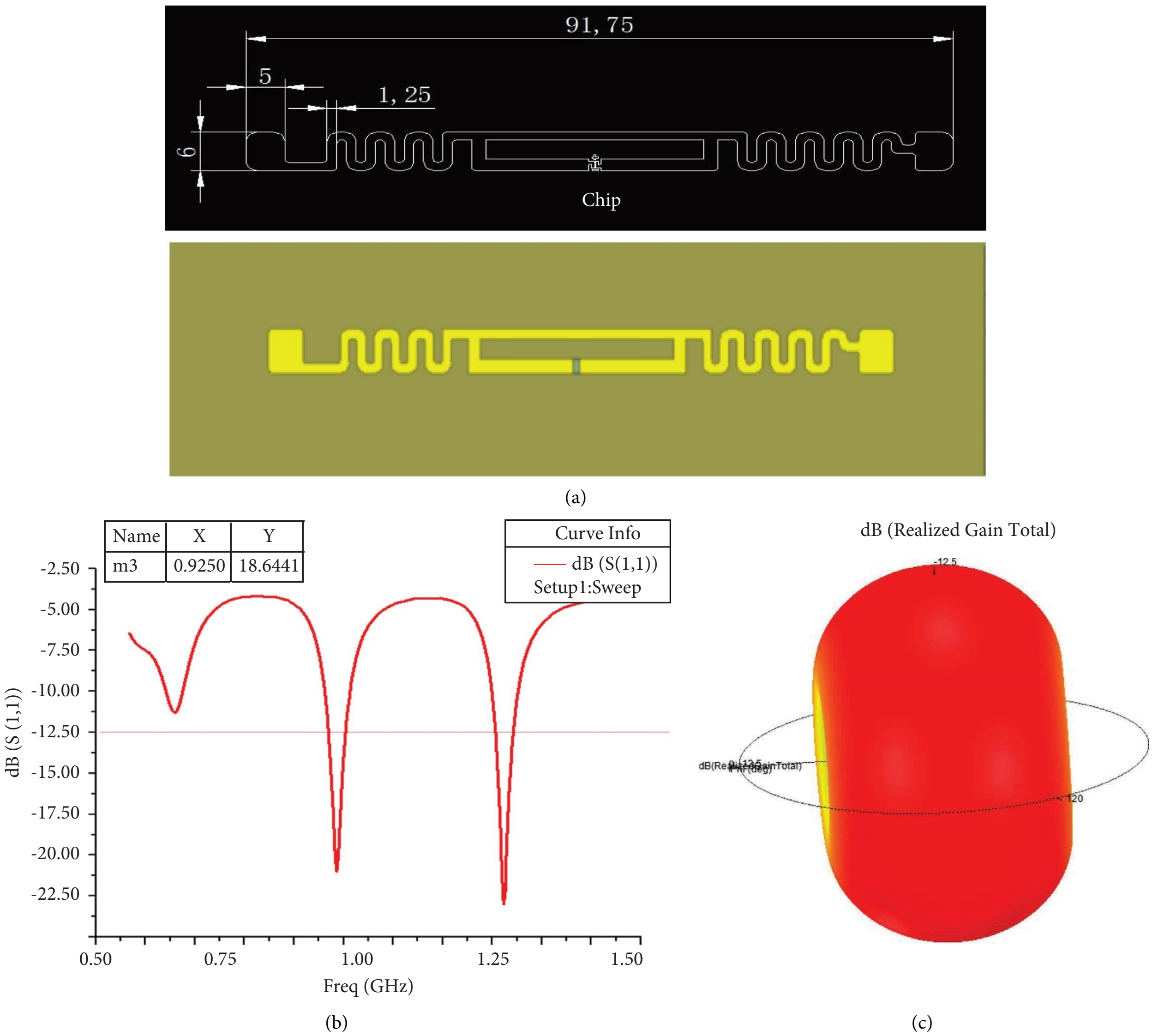

Figure 7: RFID tag antenna. (a) Measurement and simulation design model, (b) S_{11}, and (c) 3D radiation pattern.

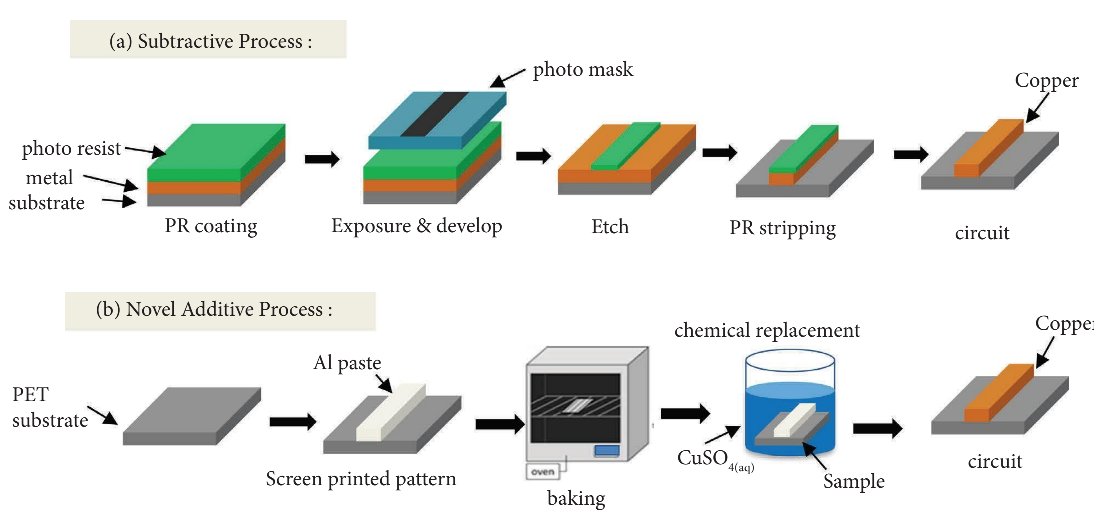

Figure 8: Comparison of process technique. (a) Subtraction process (traditional) and (b) additive process used in this work.

Table 2: Comparison table of the process technique, subtraction process (traditional) and additive process, used in this work.

Process steps	This work	Other process	This work' advantage
Process characteristics	Additive process	Subtraction process using FCCL	(i) High material utilization
Material	Flexible substrate	Flexible copper foil substrate	(i) Reduced chemical usage (ii) Low material cost
Photoresist process	None	Have	(i) Reduce CO_2 emission
Wet process	Steps: (1) Screen printing (2) Copper displacement using additives	Three steps: (1) Development (2) Etching (3) Photoresist removal	(i) Reduce >80% of consumed water and waste liquid
Chemical used in the wet process	$CuSO_4$ and H_2SO_4	Development, NaOH Etching, $CuCl_2$, HCI, NH_4Cl Photoresist removal, NaOH, inhibitor	(i) 80% less chemical used and effort for production, transportation, storage, waste treatment, and less pollutant
Resistance value	$6 \sim 12 \times 10^{-8}\ \Omega m$	$1.7 \times 10^{-8}\ \Omega m$	Sufficient conductivity for most applications

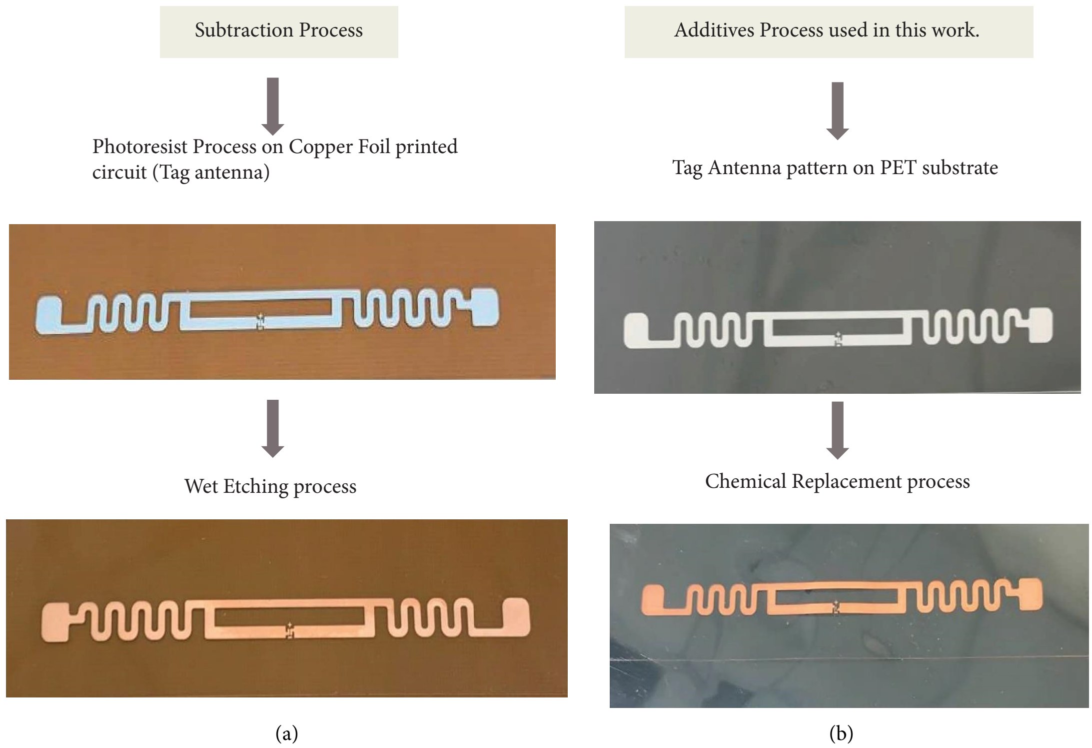

FIGURE 9: (a) The copper foil antenna fabrication by the subtractive method utilizing the etching process and (b) printed dipole antenna on a PI substrate using the additive method.

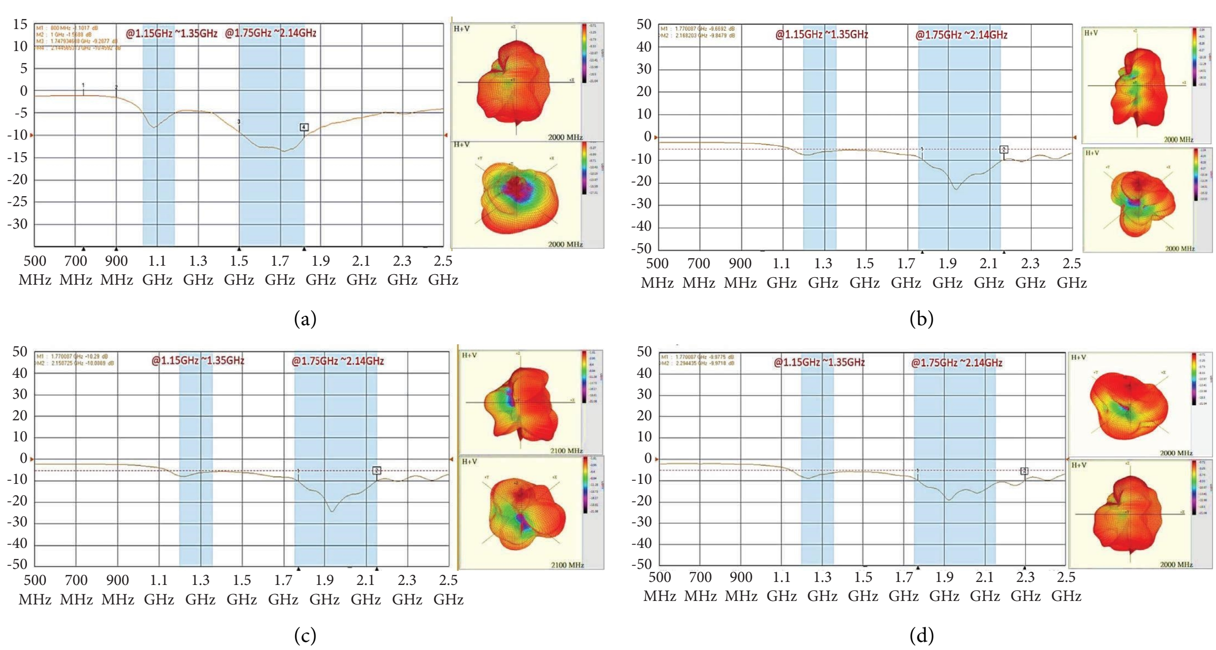

FIGURE 10: The return loss and 3D radiation pattern for (a) the copper foil antenna and the additive technique antenna at 75°C for (b) 5 minutes, (c) 10 minutes, and (d) 15 minutes.

of the anechoic chamber, the return loss, radiation pattern, and antenna efficiency of the tag antenna have been measured [15, 18]. Effective assessment of RFID module performance metrics (gain, efficiency, and read distance) necessitates specific testing methodologies. Gain is established through a comparison of emitted and received signal strengths across different distances. A controlled environment is set up, involving a calibrated RFID reader and standardized tag. Utilizing an antenna analyzer, the power radiated by the tag antenna is measured to calculate efficiency. Evaluation precision is enhanced through consistent testing, meticulous data collection, statistical analysis, and comparisons.

As per Table 3, impedance reduces with higher replacement temperatures. Figure 10 illustrates S11 antenna outcomes and 3D radiation patterns for copper foil and additive methods at 75°C for 5, 10, and 15 minutes. The analysis and evaluation of the RFID tag antenna, conducted without an IC, yield valuable insights into its behavior under varying conditions. Experiments involved copper foil and PET substrates subjected to differing temperature durations. Copper foil exhibited an impressively low 0.05 Ω impedance, indicating efficient signal transmission. Despite a slight attenuation in maximum gain (−3.5 dB), satisfactory energy conversion was evident with a maximum efficiency of −17.75%. Notably, the return loss at 1.1–1.4 GHz is less favorable for shorter replacement durations (Figure 10(b)). The growing adoption of aluminum over copper is attributed to lower proportions of the latter. Elevating copper content notably reduces return loss within specified frequency ranges. Turning to PET substrate testing, distinct patterns emerged with varying 75°C replacement durations. At 5 minutes, impedance increased to 40 Ω., signifying heightened signal resistance. While maximum gain decreased (−2.25 dB), maximum efficiency experienced marginal reduction (−18.41%). Extending replacement to 10 minutes introduced a notable alteration in signal behavior, evident in the 3.2 Ω.

Turning to PET substrate testing, distinct patterns emerged with varying 75°C replacement durations. At 5 minutes, impedance increased to 40 Ω., signifying heightened signal resistance. While maximum gain decreased (−2.25 dB), maximum efficiency experienced marginal reduction (−18.41%). Extending replacement to 10 minutes introduced a notable alteration in signal behavior, evident in the 3.2 ohm impedance and improved maximum gain (−1.97 dB). Maximum efficiency remained consistent at −18.88%. A 15-minute replacement at 75°C resulted in significant signal resistance reduction (0.826 Ω), accompanied by improved maximum gain (−1.13 dB) and a remarkable boost in maximum efficiency (−22.55%). Aluminum has mostly supplanted copper due to the low proportion of copper. Raising the copper percentage greatly reduces the return loss at 1.1–1.4 GHz and 1.7–2 GHz. While copper foil demonstrates commendable signal efficiency, PET substrate showcases impedance and gain variations with different replacement durations, impacting overall efficiency. These results provide crucial insights for optimizing RFID applications. In conclusion, evaluation of an RFID tag antenna without an integrated circuit reveals the complex relationship between substrate type, temperature, and performance.

3.2.3. RFID Tag Antenna with Schottky Diode Characteristic. RFID transponder, or tag consisting of antenna and Schottky diode (IC), was used [19, 20]. One of the key benefits of passive UHF tags is their range, which is important in numerous circumstances. However, this RFID antenna works higher than 1.26 GHz frequencies, which are occasionally referred to as microwave frequencies. Therefore, a future study will also include microwave frequencies above higher frequency RFID tags (2.45 GHz). In this frequency range, ultrahigh frequency (UHF) RFID and microwave RFID systems are commonly employed. RFID systems operating above 1.26 GHz, particularly in the UHF and microwave frequency ranges, offer enhanced capabilities for various applications. UHF RFID chips, such as the Monza R6 and Alien Higgs-3 [1, 2, 15], are commonly used in this frequency range and are connected to the antenna through precise bonding techniques to ensure a reliable connection and optimal performance.

To confirm the performance of Cu antenna fabricated by galvanic displacement, we measured the performances of tag antenna with Schottky diode. Figure 11 shows schematic images of (a) design and (b) fabricated additive antenna mounted on the standard fixture method on the fixture to reduce the environmental effect on the antenna measurement [21, 22].

Utilizing the novel additive technique on a PET substrate in accordance with the experimental analysis stated above and antenna performance, a promising result was obtained based on galvanic displacement reaction at 75°C for 15 min. Figure 12 shows the return loss and 3D radiation pattern for the copper foil antenna with Schottky diode by using the subtractive process and the antenna on PET with Schottky diode by using the novel additive process at 75°C for 15 minutes. The return loss shows that when the tag antenna is added with Schottky diode, the most obvious difference is that the model at 1.1–1.4 GHz becomes better, and the return loss at 1.1–1.4 GHz affects the gain magnitude which indirectly affects the reading distance of the tag antenna. The antenna with IC having the best performance on S_{11} is −40 dB at 1.26 GHz and −40 dB with the maximum gain of 2.87 dBi. The maximum efficiency is 53.63%. The reading distance, which represents the RFID tag antenna's propagation distance, is used to assess the performance of RFID tag with Schottky diode [22–24]. The reader used to measure the reading distance is CS461 and the transmitting antenna from convergence system limited (CSL) [25].

A comparison of the performance of the RFID tag antenna with the Schottky diode between using the copper foil with the subtractive process and using the PET film with the novel additive process at 75°C for 15 min is shown in Table 4. However, there may not be an obvious relationship between impedance and reading distance [26, 27]. The major distinction between the RFID copper foil tag antenna with Schottky diode and the RFID PET tag antenna with Schottky diode is maximum gain. Using a subtractive method, an RFID copper foil tag antenna with a Schottky diode can achieve a reading range of up to 8.5 meters. S11 has a return loss of −26 dB at 1.95 GHz and 1.21 GHz, respectively [28]. The maximum gain and efficiency are 2.24 dBi and 51.14%, respectively. In comparison to a Schottky diode substrate, the RFID PET tag antenna can be read over 9 meters further when made using an additive technique. The Schottky diode-equipped RFID PET tag antenna indicates the S11 return loss at 1.2 GHz and 2.05 GHz, respectively. The maximum gain and efficiency are 2.87 dBi and 53.63%, respectively.

Table 3: Antenna measurement result without IC.

Temperature (°C)	Time (min)	Substrate	Impedance (Ω)	Maximum gain (dBi)	Maximum efficiency (%)
Copper foil version			0.05	−3.5	17.75
75	5	PET	40	−2.25	18.41
75	10	PET	3.2	−1.97	18.88
75	15	PET	0.826	−1.13	22.55

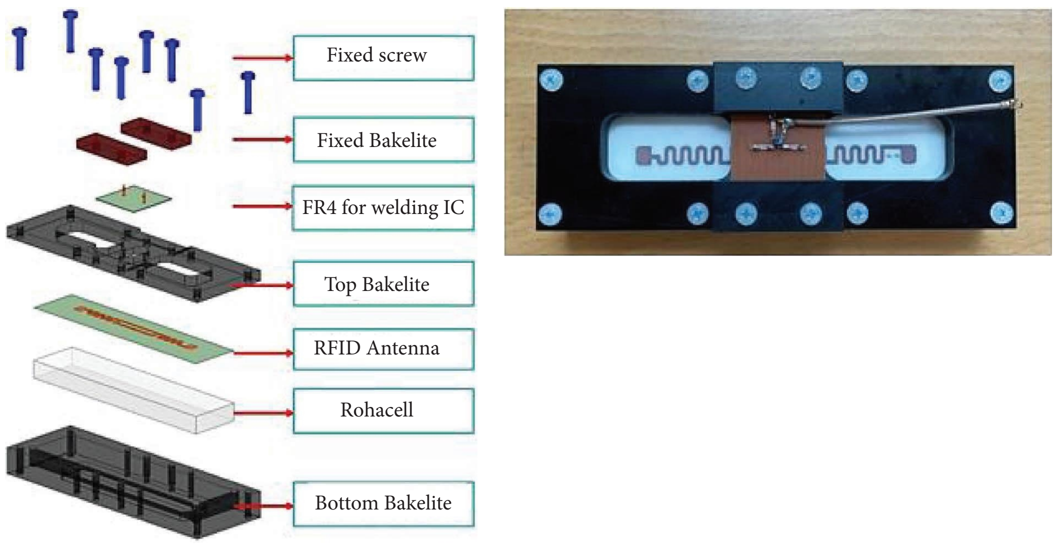

(a) (b)

Figure 11: (a) Fixture design pattern and (b) fabricated additive antenna mounted on the fixture using a standard method.

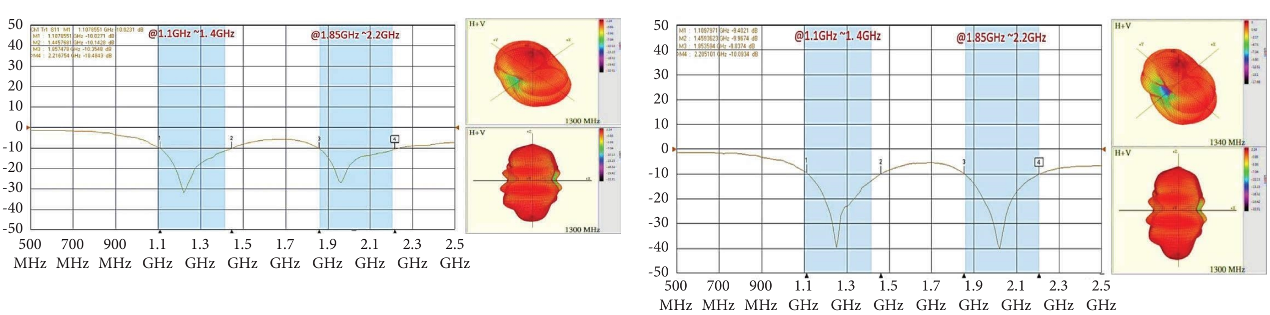

(a) (b)

Figure 12: The results of return loss and 3D radiation pattern for (a) copper foil antenna and (b) additive method antenna with Schottky diode.

Table 4: Comparison of performance for RFID tag antenna with Schottky diode by using the subtractive process and the novel additive process.

Processes	RFID copper foil sample-subtractive method	Novel additive method RFID sample at 75°C
Reading distance (m)	8.5	9
Impedance (Ω)	0.637	0.245
Maximum gain (dBi)	2.24	2.87
Maximum efficiency (%)	51.14	53.63

4. Conclusion

(1) A novel additive method for manufacturing RFID tag antennas on PET flexible substrates has been successfully developed. This method is simple, environmentally friendly, and differs from the existing subtraction process. It is based on the utilization of thick-film screen-printing aluminum pastes and galvanic replacement reaction. Future applications of this innovative RFID antenna with additive technology will incorporate into a variety of devices for information detection, collection, and asset management that can improve operational effectiveness and industries with security related applications. In addition, this additive work will be used to fabricate compact millimeter wave frequency antennas for 5G, automobile radar applications, etc.

(2) The study investigated the impact of solution temperature and immersion time on the microstructure and electrical characteristics of the aluminum electrode transformed into a copper electrode via a galvanic replacement reaction. The temperature of the solution significantly affects the size of copper grains, while the duration of immersion has a major impact on the density of the copper surface. The resistivity of the copper electrode after the galvanic replacement reaction at 75°C for 15 minutes is $2.89 \times 10^{-8}\ \Omega$m, which is comparable to that of thick film copper ($3.8 \times 10^{-8}\ \Omega$m).

(3) RFID copper foil tag antenna made by the traditional subtractive process shows that the return loss is −8 dB at 1.15–1.35 GHz, −14 dB at 1.75–2.14 GHz, and the gain, the efficiency is −3.55 dBi, 17.753%. RFID copper electrode tag antenna on the PET flexible substrate made by the novel additive method shows that the return loss S_{11} is −8 dB at 1.2 GHz, −22 dB at 1.93 GHz, and the gain, the efficiency is −2.25 dBi, 25.66%.

(4) RFID copper foil tag antenna with Schottky made by the traditional subtractive process shows that return losses are −31 dB at 1.21 GHz, −26 dB at 1.95 GHz, and gain, efficiency is 2.24 dBi, and 51.14%. The reading distance is 8.5 m. On the other hand, the RFID copper electrode tag antenna with Schottky diode on the PET substrate made by the novel additive method at 75°C for 15 min shows the return loss S_{11} of −40 dB at 1.2 6 GHz, and −40 dB at 2.05 GHz with the maximum gain is 2.87 dBi. Also, the maximum efficiency is 53.63%. The reading distance is 9 meters.

Data Availability

The data used to support the findings of this study are available from the corresponding author upon reasonable request.

Conflicts of Interest

The authors declare that they have no conflicts of interest.

Acknowledgments

This work was supported by Professor Wen-His-Lee Laboratory and the National Cheng Kung University (NCKU) of Taiwan, Ministry of Science and Technology (Taiwan).

References

[1] K. Finkenzeller, *RFID Handbook: Fundamentals and Applications in Contactless Smart Cards, Radio Frequency Identification and Near-Field Communication*, John Wiley and Sons, Hoboken, NJ, USA, 2010.

[2] S. Winder and J. Carr, *Newnes Radio and RF Engineering Pocketbook*, Newnes, Boston, MA, USA, 2002.

[3] G. Rt White, G. Gardiner, G. P. Prabhakar, and A. Abd Razak, "A comparison of barcoding and RFID technologies in practice," *Journal of information, information technology and organizations*, vol. 2, pp. 119–132, 2007.

[4] W. S. Suh, E. J. Yoon, and S. Piramuthu, "RFID-based attack scenarios in retailing, healthcare and sports," *Journal of Information Privacy and Security*, vol. 9, no. 3, pp. 4–17, 2013.

[5] C.-H. Tsai, Y.-H. Shen, and W.-T. Tsai, "Sustainable material management of industrial hazardous waste in Taiwan: case studies in circular economy," *Sustainability*, vol. 13, no. 16, p. 9410, 2021.

[6] N. V. Mdlovu, C.-L. Chiang, K.-S. Lin, and R.-C. Jeng, "Recycling copper nanoparticles from printed circuit board waste etchants via a microemulsion process," *Journal of Cleaner Production*, vol. 185, pp. 781–796, 2018.

[7] A. Ibitz, "Assessing Taiwan's endeavors towards a circular economy: the electronics sector," *Asia Europe Journal*, vol. 18, no. 4, pp. 493–510, 2020.

[8] M. S. Islam, A. Maher, M. A. Hannan, and B. Hasan, "Overview for solid waste bin monitoring and collection system," in *Proceedings of the 2012 International Conference on Innovation Management and Technology Research*, pp. 258–262, IEEE, Malacca, Malaysia, May 2012.

[9] T. C. Kuo, C. R. Kuo, W. H. Lee, and W.-H. Lee, "A novel method to fabricate a thick-film Cu electrode fired in air through printing Al electrode and reduction-oxidation substitution reaction," *IEEE Transactions on Components, Packaging, and Manufacturing Technology*, vol. 11, no. 3, pp. 485–492, 2021.

[10] R. Thota, S. Sundari, S. Berchmans, and V. Ganesh, "Silver‐copper bimetallic flexible electrodes prepared using a galvanic replacement reaction and their applications," *ChemistrySelect*, vol. 2, no. 6, pp. 2114–2122, 2017.

[11] D. A. Brevnov, T. S. Olson, G. P. López, and P. Atanassov, "Electroless deposition of silver by galvanic displacement on aluminum alloyed with copper," *The Journal of Physical Chemistry B*, vol. 108, no. 45, pp. 17531–17536, 2004.

[12] J. Liu, C. Yang, P. Zou et al., "Flexible copper wires through galvanic replacement of zinc paste: a highly cost-effective technology for wiring flexible printed circuits," *Journal of Materials Chemistry C*, vol. 3, no. 32, pp. 8329–8335, 2015.

[13] R. Colella, F. P. Chietera, F. Montagna, A. Greco, and L. Catarinucci, "On the use of additive manufacturing 3D-printing technology in RFID antenna design," in *Proceedings of the 2019 IEEE International Conference on RFID Technology and Applications (RFID-TA)*, pp. 433–438, IEEE, Pisa, Italy, September 2019.

[14] J. M. Felício, A. Sérgio, J. R. C. A. M. A. Matos, and C. A. Fernandes, "Wrist-worn RFID antenna printed on additive manufactured flexible substrate," in *Proceedings of*

the 2019 IEEE International Symposium on Antennas and Propagation and USNC-URSI Radio Science Meeting, pp. 83-84, IEEE, Atlanta, GA, USA, July 2019.

[15] C. M. Roberts, "Radio frequency identification (RFID)," *Computers and Security*, vol. 25, no. 1, pp. 18–26, 2006.

[16] H. He, "New Additive Manufacturing Solutions and Novel Materials for UHF RFID Tag Antennas and Interconnections," 2018, https://cris.tuni.fi/ws/portalfiles/portal/15836836/he_1550.pdf.

[17] J. Li, H. Liu, S. Zhang, M. Luo, Y. Zhang, and S. He, "A wideband single-fed, circularly-polarized patch antenna with enhanced axial ratio bandwidth for UHF RFID reader applications," *IEEE Access*, vol. 6, pp. 55883–55892, 2018.

[18] G. G. Xiao, Z. Zhang, S. Lang, and T. Ye, "Screen printing RF antennas," in *Proceedings of the 2016 17th International Symposium on Antenna Technology and Applied Electromagnetics (ANTEM)*, pp. 1-2, IEEE, Montreal, Canada, July 2016.

[19] A. M. J. Marindra, P. Pongpaibool, W. Wallada, and S. Siwamogsatham, "An optimized ink-reducing hollowed-out arm meander dipole antenna structure for printed RFID tags," *International Journal of Microwave and Wireless Technologies*, vol. 9, no. 2, pp. 469–479, 2017.

[20] W. Yang, X. Cheng, Z. Guo, Q. Sun, J. Wang, and C. Wang, "Design, fabrication and applications of flexible RFID antennas based on printed electronic materials and technologies," *Journal of Materials Chemistry C*, vol. 11, no. 2, pp. 406–425, 2023.

[21] J. J. Kelly and A. C. West, "Copper deposition in the presence of polyethylene glycol: I. Quartz crystal microbalance study," *Journal of the Electrochemical Society*, vol. 145, no. 10, pp. 3472–3476, 1998.

[22] J. P. Healy, D. Pletcher, and M. Goodenough, "The chemistry of the additives in an acid copper electroplating bath: Part II. The instability 4, 5-dithiaoctane-1, 8-disulphonic acid in the bath on open circuit," *Journal of Electroanalytical Chemistry*, vol. 338, no. 1-2, pp. 167–177, 1992.

[23] E. Sipilä, "Novel Manufacturing Methods and Materials for UHF RFID Tags in Identification and Sensing Applications," 2016, https://trepo.tuni.fi/handle/10024/114814.

[24] S. F. Jilani and A. Alomainy, "Planar millimeter-wave antenna on low-cost flexible PET substrate for 5G applications," in *Proceedings of the 2016 10th European Conference on Antennas and Propagation (EuCAP)*, pp. 1–3, IEEE, Davos, Switzerland, April 2016.

[25] G. A. Casula, G. Montisci, G. Mazzarella, and M. Giuseppe, "A wideband PET inkjet-printed antenna for UHF RFID," *IEEE Antennas and Wireless Propagation Letters*, vol. 12, pp. 1400–1403, 2013.

[26] D. Betancourt and J. Castan, "Printed antenna on flexible low-cost PET substrate for UHF applications," *Progress in Electromagnetics Research C*, vol. 38, pp. 129–140, 2013.

[27] P. Fathi, S. Shrestha, R. Yerramilli, N. Karmakar, and S. Bhattacharya, "Screen printed chipless RFID tags on packaging substrates," *Flexible and Printed Electronics*, vol. 6, no. 2, Article ID 025009, 2021.

[28] S. Bhaskar and A. K. Singh, "A Compact meander line UHF RFID antenna for passive tag applications," *Progress in Electromagnetics Research M*, vol. 99, pp. 57–67, 2021.